









Proceedings Article

First Complex Trials Using a Dedicated Balloon Catheter for Magnetic Particle Imaging

Patryk Szwargulski ^{a,b,c,*} · Tobias Knopp ^{a,b,c} · Marija Boberg ^{a,b,c} · Johannes Salamon ^c · Vincent Scheitenberger ^d · Thorsten Götttsche ^d · Reinhard Linemann ^e · Franz Wegner ^f · Thomas Friedrich ^{g,h} · Jörg Barkhausen ^f · Thorsten M. Buzug ^{g,h} · Mandy Ahlberg ^{g,h}

^aSection for Biomedical Imaging, University Medical Center Hamburg-Eppendorf, Hamburg, Germany

^bInstitute for Biomedical Imaging, Hamburg University of Technology, Hamburg, Germany

^cDepartment for Diagnostic and Interventional Radiology and Nuclear Medicine, University Medical Center Hamburg- Eppendorf, Hamburg, Germany

^dOsypka AG, Rheinfelden, Germany

^eEvonik Operations GmbH, Marl, Germany

^fDepartment of Radiology and Nuclear Medicine, University of Lübeck, Lübeck, Germany

^gFraunhofer Research Institution for Individualized and Cell-Based Medical Engineering, Lübeck, Germany

^hInstitute of Medical Engineering, Universität zu Lübeck, Lübeck, Germany

*Corresponding author, email: p.szwargulski@uke.de

© 2021 Szwargulski *et al.*; licensee Infinite Science Publishing GmbH

This is an Open Access article distributed under the terms of the Creative Commons Attribution License (<http://creativecommons.org/licenses/by/4.0>), which permits unrestricted use, distribution, and reproduction in any medium, provided the original work is properly cited.

Abstract

A recent work introduced a balloon catheter from a polymer mixed with magnetic nanoparticles that was visible in magnetic particle imaging (MPI) in initial trials. In this work, dynamic multi-patch and multi-contrast experiments were performed to validate the applicability of the balloon catheter for complex application scenarios in MPI. In both cases, the balloon was successfully imaged, although there are limitations in resolution and dynamic imaging range.

I. Introduction

On the way bringing magnetic particle imaging (MPI) with its huge potential into the clinic multiple steps are necessary. Next to the hardware [1], the imaging sequence [2], and the tracer material [3] also the compatibility of interventional devices is an important field of research. Recently, the first quasi-commercial interventional balloon catheter (prototype that fulfills all standards for commercial catheters) for MPI has been presented [4]. While in the previous work the main focus was on the fabrication and characterization, in this work

advanced imaging sequences are evaluated. First, if the balloon catheter can be imaged completely and artifact-free using a multi-patch sequence. Second, if the balloon catheter can be distinguished from other materials, such as liquid tracer. Both questions are of utmost relevance for the applicability of the balloon catheter in practice.

II. Methods and Materials

A picture of the balloon catheter is shown in Figure 1. The used balloon was developed using magnetic nanoparti-



Figure 1: Picture of the balloon catheter together with a sketch of the measurement areas used in the multi-patch experiment.

cles of the product series MagSilica[®] (Evonik Industries AG, Essen, Germany) and a polymer of the product series VESTAMID[®] (Evonik Industries AG, Essen, Germany). In this proof of concept trial a balloon with a nanoparticle proportion of 30 wt% has been validated. Further information on the balloon catheter and its manufacture process is reported in [4].

III. Experiments

In this study, we performed two dynamic 3D MPI experiments using the preclinical Bruker MPI System 25/20FF [5] (Bruker BioSpin MRI GmbH, Ettlingen, Germany) with an additional dedicated receive coil [6]. On the one hand, a multi-patch experiment [7] and on the other hand, a multi-contrast experiment [8] were carried out. All measurements were performed using a gradient strength of 2 T m^{-1} and a drive field strength of 12 mT resulting in a covered field of view (FoV) of $24 \times 24 \times 12 \text{ mm}^3$. For reconstruction the open-source Julia package MPIReco.jl [9] was used.

Multi-Patch Experiment

The first experiment was a dynamic multi-patch experiment to visualize the entire balloon using two patches. The balloon catheter and the multi-patch positions are shown in Figure 1. The scan protocol included pulling the balloon into the scanner, inflating and deflating it and finally pulling it out of the scanner. The scan time was about 2.5 min. The imaging sequence consisted of a repetitive scanning of two patches with a repetition time of about 1 s including 20 static and 4 shifting frames per patch. The two patches had an overlap of 2 mm in x -direction and covered together a FoV of $46 \times 24 \times 12 \text{ mm}^3$. For each patch an individual system matrix was measured to avoid potential artifacts due to field inhomogeneities.

For the joint reconstruction of a frame, the data of temporally adjacent patches were combined [10]. In addition, 20 frames per patch were averaged to increase the signal-to-noise ratio (SNR).

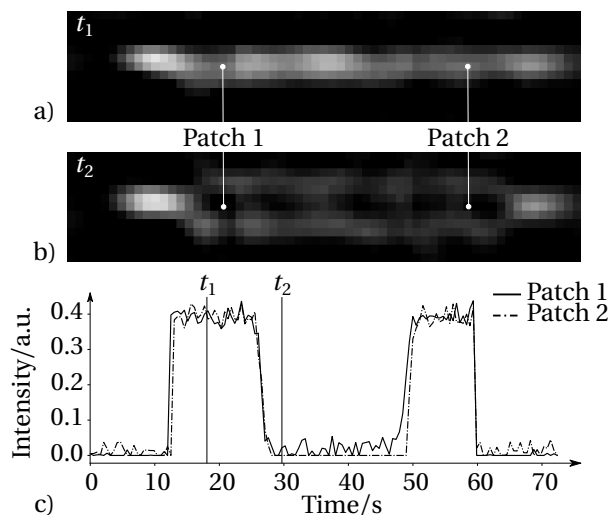


Figure 2: Results of the multi-patch experiment. The xz -view of the balloon catheter is shown in the deflated (a) and inflated state (b). In c) the normalized signal from the marked positions of both patches is shown over time. For normalization the maximum intensity of the reconstructed image was used.

Multi-Contrast Experiment

The second experiment was a dynamic multi-contrast experiment to showcase the possibility of separating the balloon and liquid perimag (micromod Partikeltechnologie GmbH, Rostock, Germany). During the experiment we placed the balloon catheter into the FoV followed by inserting a $5 \mu\text{l}$ diluted perimag sample. The concentration of the sample was $170 \text{ ng}_{\text{Fe}} \mu\text{l}^{-1}$. After the visualization of both, the balloon and the sample, the balloon was first inflated and after a few seconds deflated followed by removing everything from the FoV. For the balloon and perimag individual system matrices on the same grid of size $25 \times 25 \times 13$ with a voxel size of $1 \times 1 \times 1 \text{ mm}^3$ were measured.

IV. Results

Multi-Patch Results

The results of the multi-patch experiment are shown in Figure 2. A xz -slice of the reconstructed balloon catheter at two different times (t_1, t_2) is shown in a) and b). In c) the signal intensities at the center of the reconstructed patches marked with a white dot are shown. It is clearly visible that both curves are almost identical and there are no inconsistencies in the synchronization and reconstruction of the data. The different states of the experiment can also be observed in the course of the signal intensities.

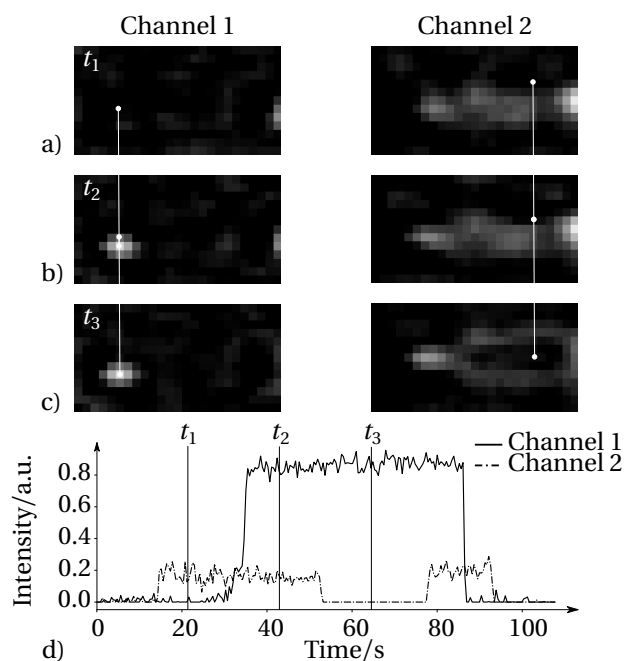


Figure 3: Results of the multi-contrast experiment. Both channels at three points in time are shown. The channel for the perimag sample is shown on the left and the channel for the balloon catheter on the right. In d) the normalized signal from the marked positions of both channels is shown over time. For normalization the maximum intensity of the reconstructed image was used.

Multi-Contrast Results

The results of the multi-contrast experiment are presented in Figure 3, which shows an xz -view for both channels. In a)-c) the reconstruction result of three subsequent time points are shown. Each time point shows a new phase of the experiment. Thus in a) only the balloon is visible, while in b) and c) the perimag sample and the deflated and inflated balloon is shown, respectively. In each case, the sample is clearly separable from the balloon catheter. In d) the intensity curve per channel from the reconstructed images is presented. The locations at which the intensity profile was taken are marked with a white dot. Additionally, the different phases of the experiment can be read from the intensity curve. As can be clearly seen, there is no signal leakage between both channels, which indicates good separability.

V. Discussion

As shown in the results, a successful reconstruction of the balloon catheter is possible in multi-patch and multi-contrast experiments. Regarding the image quality, one has to note that the experiments carried out here were performed with a dedicated receiver coil that has a significantly higher sensitivity compared to the system's own

coils.

The multi-patch experiments will be necessary in future applications since the relatively small FoV of the excitation field will not be sufficient to display the entire balloon catheter. An alternative could be the reduction of the gradient or the use of multi-gradient approaches [11]. It remains to be verified at which gradient the balloon can still be recognized as such in the inflated state. In our case, it was already difficult to successfully reconstruct the balloon walls in the orthogonal direction.

The multi-contrast test showed that the developed balloon catheter can be separated well from the liquid perimag. This is very important, since an application scenario is conceivable in which a (blood pool) tracer was injected into the patient prior to the examination and requires a clear separation from the balloon catheter for navigation. However, the influence of different tracer concentrations in presence of the balloon catheter on the reconstruction should be further investigated.

VI. Conclusion

In this work, dynamic experiments showed that the quasi-commercial balloon catheter developed in [4] is suitable for multi-patch and multi-contrast imaging. In multi-patch imaging, an artifact-free and true-size reconstruction of the entire balloon was possible. With multi-contrast reconstruction, a clear separation of the balloon from the liquid tracer material was feasible. In summary, the quasi-commercial balloon catheter is very promising for interventional applications and would be suitable for first application-oriented in-vitro and in-vivo studies that will involve the multi-patch and multi-contrast imaging techniques evaluated in this work.

Acknowledgments

The authors acknowledge funding of the study by the Federal Ministry of Education and Research (BMBF) under grant numbers 13GW0071D (M. Ahlborg, T. Buzug, T. Friedrich), 13GW0071A (R. Linemann) and 13GW0071B (T. Göttsche, V. Scheitenberger).

Author's statement

Conflict of interest: Authors state no conflict of interest.

References

- [1] M. Graeser, F. Thieben, P. Szwargulski, F. Werner, N. Gdaniec, M. Boberg, F. Griesse, M. Möddel, P. Ludewig, D. van de Ven, O. M. Weber, O. Woywode, B. Gleich, and T. Knopp. Human-sized magnetic particle imaging for brain applications. *Nature Communications*, 10(1), 2019, doi:10.1038/s41467-019-09704-x.

- [2] T. Knopp, N. Gdaniec, and M. Möddel. Magnetic particle imaging: From proof of principle to preclinical applications. *Physics in Medicine and Biology*, 62(14):R124–R178, 2017, doi:[10.1088/1361-6560/aa6c99](https://doi.org/10.1088/1361-6560/aa6c99).
- [3] C. Grüttner, A. Kowalski, F. Fidler, M. Steinke, F. Westphal, and H. Teller. Synomag® nanoflower particles: A new tracer for MPI, physical characterization and initial invitro toxicity studies, in *International Workshop on Magnetic Particle Imaging*, 17–18, 2018.
- [4] M. Ahlborg, T. Friedrich, T. Götttsche, V. Scheitenberger, R. Lineemann, M. Wattenberg, A. T. Büssen, T. Knopp, P. Szwargulski, M. Kaul, J. Salamon, T. M. Buzug, J. Barkhausen, and F. Wegner. A dedicated balloon catheter for magnetic particle imaging. *International Journal on Magnetic Particle Imaging*, 8, 2022.
- [5] MPI - Bruker's revolutionary modality for preclinical imaging, https://www.bruker.com/en/products-and-solutions/preclinical-imaging/mpi/_jcr_content/root/sections/highlights/sectionpar/highlightfacts.download-asset.pdf/items/374_1586262213721/link/mppi_preclinical_T149457.pdf, Online; access 09.09.2021.
- [6] M. Graeser, T. Knopp, P. Szwargulski, T. Friedrich, A. Von Gladiss, M. Kaul, K. M. Krishnan, H. Ittrich, G. Adam, and T. M. Buzug. Towards picogram detection of superparamagnetic iron-oxide particles using a gradiometric receive coil. *Scientific Reports*, 7(1):6872, 2017, doi:[10.1038/s41598-017-06992-5](https://doi.org/10.1038/s41598-017-06992-5).
- [7] B. Gleich, J. Weizenecker, H. Timminger, C. Bontus, I. Schmale, J. Rahmer, J. Schmidt, J. Kanzenbach, and J. Borgert. Fast MPI demonstrator with enlarged field of view, in *Proc. ISMRM*, 18, 218, Stockholm, 2010.
- [8] J. Rahmer, A. Halkola, B. Gleich, I. Schmale, and J. Borgert. First experimental evidence of the feasibility of multi-color magnetic particle imaging. *Physics in medicine and biology*, 60(5):1775–1791, 2015, doi:[10.1088/0031-9155/60/5/1775](https://doi.org/10.1088/0031-9155/60/5/1775).
- [9] T. Knopp, P. Szwargulski, F. Griese, M. Grosser, M. Boberg, and M. Möddel. MPIReco.jl: Julia package for image reconstruction in MPI. *International Journal on Magnetic Particle Imaging*, 5(1), 2019, doi:[10.18416/ijmpi.2019.1907001](https://doi.org/10.18416/ijmpi.2019.1907001).
- [10] N. Gdaniec, M. Boberg, M. Möddel, P. Szwargulski, and T. Knopp. Suppression of motion artifacts caused by temporally recurring tracer distributions in multi-patch magnetic particle imaging. *IEEE transactions on medical imaging*, 39(11):3548–3558, 2020, doi:[10.1109/TMI.2020.2998910](https://doi.org/10.1109/TMI.2020.2998910).
- [11] N. Gdaniec, P. Szwargulski, and T. Knopp. Fast multi-resolution data acquisition for magnetic particle imaging using adaptive feature detection: *Medical Physics*, 44(12):6456–6460, 2017, doi:[10.1002/mp.12628](https://doi.org/10.1002/mp.12628).